

Probing the Therapeutic Efficacy of *Combretum paniculatum* Extract and GC-FID-Identified Phytochemicals as Novel Agents for Diabetes Mellitus

Bioinformatics and Biology Insights
Volume 18: 1–15
© The Author(s) 2024
Article reuse guidelines:
sagepub.com/journals-permissions
DOI: 10.1177/11779322241271537



Ifeoma F Chukwuma^{1,2}, Chidi E Atikpoh¹ , Victor O Apeh³ ,
Florence N Nworah^{1,2} and Lawrence US Ezeanyika¹

¹Department of Biochemistry, Faculty of Biological Sciences, University of Nigeria, Nsukka, Nigeria. ²Department of Genetics and Biotechnology, Faculty of Biological Sciences, University of Nigeria, Nsukka, Nigeria. ³Department of Applied Sciences, Federal University of Allied Health Sciences, Enugu, Nigeria.

ABSTRACT

OBJECTIVES: Oxidative stress is implicated in several metabolic cascades involved in glucose control. Hence, investigating antioxidant and antidiabetic activities is crucial for discovering an effective diabetes mellitus (DM) agent. This study was aimed at probing the therapeutic efficacy of hydro-ethanolic extract of *Combretum paniculatum* (HECP) and gas chromatography-flame ionization detector (GC-FID)-identified phytochemicals as novel agents for DM.

METHODS: We determined the total phenols, flavonoids, and antioxidant vitamins in HECP using standard methods. A GC-FID was used to decipher phytochemicals of HECP. The antioxidant and antidiabetic activities of HECP were assessed using in vitro and in silico approaches.

RESULTS: The results revealed that HECP is affluent in phenols, flavonoids, and vitamin E and demonstrated engaging antioxidant activities in 1,1-diphenyl-2-picryl-hydroxyl (DPPH; $IC_{50} = 0.83 \mu\text{g/mL}$), thiobarbituric acid-reactive substances TBARS; $IC_{50} = 2.28 \mu\text{g/mL}$, and ferric-reducing antioxidant power assay (FRAP; $IC_{50} = 2.89 \mu\text{g/mL}$). Compared with the reference drug, acarbose, HECP exhibited good α -amylase and α -glucosidase inhibitory capacity, having IC_{50} values of 14.21 and 13.23 $\mu\text{g/mL}$, respectively, against 13.06 and 11.71 $\mu\text{g/mL}$ recorded for acarbose. More so, the extract's top 6 scoring phytochemicals (rutin, kaempferol, epicatechin, ephedrine, naringenin, and resveratrol) had strong interactions with amino acid residues within and around α -amylase and α -glucosidase active site domains. All the compounds but rutin had favourable drug-like characteristics, pharmacokinetics, and safety profiles when compared with acarbose.

CONCLUSION: Altogether, our results vindicate the use of this herb in treating DM locally and reveal that it has pharmaceutically active components that could be used as novel leads in the development of DM drugs.

KEYWORDS: α -Amylase, α -glucosidase, ADMET properties, antioxidants, diabetes, *Combretum paniculatum*, in silico

RECEIVED: August 31, 2023. ACCEPTED: June 3, 2024.

TYPE: Research Article

FUNDING: The author(s) received no financial support for the research, authorship, and/or publication of this article.

DECLARATION OF CONFLICTING INTERESTS: The author(s) declared no potential conflicts of interest with respect to the research, authorship, and/or publication of this article.

CORRESPONDING AUTHOR: Ifeoma F Chukwuma, Department of Biochemistry, Faculty of Biological Sciences, University of Nigeria, Nsukka 410001, Enugu State, Nigeria. Email: chukwuma.ifeoma@unn.edu.ng; odoifeoma1@gmail.com

Introduction

Diabetes mellitus (DM) accounts for approximately 4.9 million deaths globally.¹ Recently, reports by the International Diabetes Federation (IDF) show that 463 million people worldwide have diabetes in 2019, with a dismal prediction that this number will increase to 700.2 million by 2045.² Consequently, DM's substantial economic, social, and health complications make it a global challenge requiring urgent attention.³ DM is, among others, caused by aberrations in the immune network culminating in macrophage, CD4+, and CD8+ T-cell autoimmune destruction of pancreatic cells, leading to insulin deficiency (type 1 diabetes). The decrease in insulin secretion and resistance are the fundamental mechanisms involved in the etiopathogenesis of type 2 diabetes (T2D).⁴ A third classification, gestational DM, arises when hormonal changes in pregnancy step up the blood glucose

level.⁵ In light of this, deregulated blood glucose levels in all types of DM provoke dyslipidemia, hypertension, and, ultimately, several organ damages, leading to polyphagia, polyuria, retinopathy, neuropathy, nephropathy, and atherosclerosis.¹ In addition, patients with DM are more susceptible to liver, pancreas, breast, stomach, urinary bladder, and lymphoid tissue cancer.⁶ The biochemical pathways mediating increased risk of cancer and other related secondary diseases in patients with DM are activated by an unregulated inflammatory response, insulin resistance, hyperinsulinemia, and oxidative stress.^{6,7}

According to experimental findings, oxidative stress plays a significant role in the aetiology and pathogenesis of all kinds of DM, possibly because sustained hyperglycaemia overloads the electron transport chain by generating excess NADH and FADH₂.³ It is worth mentioning that the increased supply of NADH and FADH₂ in diabetes is contributed not only



Creative Commons Non Commercial CC BY-NC: This article is distributed under the terms of the Creative Commons Attribution-NonCommercial 4.0 License (<https://creativecommons.org/licenses/by-nc/4.0/>) which permits non-commercial use, reproduction and distribution of the work without

further permission provided the original work is attributed as specified on the SAGE and Open Access pages (<https://us.sagepub.com/en-us/nam/open-access-at-sage>).

by oxidation of glucose but also by hyperglycaemia-mediated activation of gluconeogenesis, protein, and fatty acid oxidations.⁸ This initiates aberrant production of superoxide radicals and other free radical species above tolerable or physiological concentrations, which disrupts the redox equilibrium. The increase in oxidant species may cause or contribute to the development of oxidative damage via DNA damage, leading to the activation of poly-ADP-ribose polymerase (PARP).⁹ The activated PARP will, in turn, inhibit the activity of glyceraldehyde-3-phosphate dehydrogenase (GA3PDG), which leads to the accumulation of glycolysis intermediates and subsequent activation of pro-oxidant pathways such as polyol and hexosamine pathways, protein kinase C (PKC) activity, and formation of advanced glycation end-products (AGEs).^{10,11} Besides this, oxidative stress provokes the development of T2D through the involvement of nuclear factor kappa B, protein kinase p53, Mitogen-activated protein kinases (MAPK), and NH₂-terminal Jun kinases, which may interfere with insulin signalling pathways, destroying pancreatic β -cells and insulin resistance.¹² The excess oxidant species may decrease insulin release by deteriorating the pancreas's islet cells and, by extension, elicit several micro- and macrovascular diabetic complications that are responsible for the long-term disability and death of patients.^{2,12,13} It is worth mentioning that the high susceptibility of the pancreatic islets to reactive oxygen species (ROS) is mainly due to their low expression of redox-regulating enzymes and free radical detoxifying enzymes.³ In light of this, antioxidant enzymes are usually altered in patients with T2D.³ Consequently, antioxidants are considered important therapeutic agents for preventing the pathogenesis of DM and pancreatic tissue damage.¹⁴

Accordingly, the World Health Organization (WHO) expert committee on diabetes has recommended screening medicinal plants to improve the normal glycaemic and antioxidant status and prevent the destruction of pancreatic β -cells and other diabetic-mediated anomalies.² Conversely, there is now bench-to-bedside investigation to identify anti-DM agents from medicinal plants or natural products that could be used in clinical settings and also to identify their pharmacologically active compounds, which may potentially serve as a lead agent for drug development and applications. Medicinal plants contain a repository of multi-component bioactive compounds that have demonstrated astounding therapeutic activity with a multi-targeted approach compared with single-component treatments. Moreover, they have a better safety profile, are cheaper alternatives, and are accessible and biocompatible.^{15,16} Interestingly, emerging research evidence has registered the therapeutic efficacy of several medicinal plants against DM, but several other plants, including *Combretum paniculatum*, are yet to be explored.

Combretum paniculatum is a member of the Combretaceae family and a wild plant of African origin that is now widely distributed on other continents. It is commonly called burning bush or forest flame-creeper in English. The plant components

were historically used in African civilization as food, medicine, and ornamentation. The plant is embraced for several ethnomedicinal purposes as remedies for diarrhoea, chronic dysentery, flatulence, enlarged liver, stomach pain, wounds, stomatitis, ringworm, gonorrhoea, leprosy, and eye diseases.¹⁷ *Combretum paniculatum* has demonstrated numerous pharmacological potentials, including antimicrobial, anti-trypanocidal, anti-cancer, anti-viral, and antidiabetic activities.^{17,18} The anti-inflammatory and toxicity profile of the extract has been appraised.¹⁷ Herein, we investigate the chemical composition of the extract. Panels of in vitro therapeutic targets fundamental to metabolic changes in diabetes, namely the potential to manage oxidative stress through antioxidant action and inhibition of carbohydrate metabolizing enzymes (α -glucosidase and α -amylase), were employed to appraise the antidiabetic potential of hydro-ethanolic extract of *Combretum paniculatum* (HECP). Furthermore, in silico studies via molecular docking, drug-likeness, pharmacokinetics, and toxicity screening were used to explore the therapeutic value and safety profile of the gas chromatography-flame ionization detector (GC-FID)-identified phytochemicals as potent DM antagonists.

Materials and Methods

Identification, collection, and preparation of Combretum paniculatum hydro-ethanolic extract

Fresh *C. paniculatum* leaves were collected from Nsukka Local Government Area, Enugu State Nigeria, and an expert, Mr. Alfred Ozioko, made taxonomic identification. A voucher specimen of the leaves with reference number InterCEDD/1909 was deposited in the herbarium of the International Centre for Ethnomedicine and Drug Development (InterCEDD) in Nsukka, Enugu State, Nigeria. The obtained leaves were air-dried at room temperature, ground (11205 g), and then immersed in 5.6 L of distilled water-ethanol (30:70 v/v) for 3 days while being shaken occasionally. The macerate was filtered and concentrated with a vacuum rotary evaporator (R-215, Buchi, Flawil, Switzerland) under reduced pressure and at a temperature of 45°C. Until needed, the hydro-ethanolic extract of *C. paniculatum* (HECP) was stored at 4°C in an airtight screw-capped bottle.

Chemicals and reagents

The experiments were conducted with these analytical-grade chemicals and reagents: Aluminium chloride, ascorbic acid, α -amylase, 2,2-diphenyl-1-picrylhydrazyl, ethanol, ethyl acetate, ferric chloride, folin ciocalteau's reagent, gallic acid, α -glucosidase, and quercetin were products of Sigma-Aldrich, Inc., UK. While a-a 1-dipyridyl, diethyl ether, diphenol indo 2, 6-dichlorophenol, iron (II) tetraoxosulphate (IV), methanol, n-hexane, potassium acetate, sodium sulphate, and sodium bicarbonate were products of British Drug Houses (BDH) Chemicals Ltd., Poole, England.

Total phenol content. The total phenols present in HECP were quantified using the Singleton and Rossi¹⁹ procedure. Equal volumes (1.5 mL) of HECP and 1/10 dilution of folin-ciocal-teau reagent were added to 2% sodium carbonate (1.5 mL w/v), and the resultant mixture was incubated at 45°C for 15 minutes. Finally, the absorbance was taken at 765 nm using a UV/visible spectrophotometer (Jenway 6305, Bibby Scientific Ltd., UK). Total phenol content (TPC) was reported using the gallic acid equivalent (GAE) value.

Total flavonoid content. The total flavonoid content (TFC) of HECP computed in quercetin equivalent (QE) value was ascertained following the Zhishen et al²⁰ method. A mixture of the extract (0.5 mL), aluminium chloride (0.2 mL), 1M potassium acetate (0.2 mL), and distilled water (5.6 mL) was incubated for 30 minutes before measuring absorbance at 415 nm.

Estimation of vitamin A content. The extract was freshly prepared according to the Association of Official Analytical Chemist (AOAC)²¹ methodology, and it was added to 10 mL of isopropanol before measuring for extinction at 325 nm compared with a solvent blank (T1) to assess the total amount of vitamin A in HECP. The cuvettes were subsequently taken out and placed under ultraviolet (UV) radiation till the extinction stopped decreasing with time; at this point, the absorbance was measured again (T2). The ST1 and ST2 of the standard vitamin A solution were determined by performing the same procedure. The concentration of vitamin A was obtained with Equation 1.

$$\text{Vitamin A (mg / 100 g)} = \frac{T1 - T2}{ST1 - ST2} \times 1 \times \text{Dilution factor} \quad (1)$$

Determination of vitamin C. The amount of vitamin C in HECP was measured using DPIP (diphenol indo 2,6,-dichlorophenol) titration following the AOAC²¹ method. Sodium bicarbonate (100 mg/L) and DPIP (295 mg/L) were titrated using 0.2 g of HECP and 4 mL of oxalic acid (1 g/L) and sodium acetate (4 g/L) buffer solution. The following equation (Equation 2) was used to determine the amount of vitamin C in the samples:

$$\text{Vitamin C (mg / 100 g)} = \frac{MV \times 100 \times 100}{10B} \quad (2)$$

where M = titration mass of ascorbic acid equivalent to 0.001 M DPIP solution (mg); V = titrant volume of 0.001 M DPIP solution (mL); 100 x 100 stands for the dilution ratio of the sample and the conversion scaling factor per 100 g of raw materials, respectively; 10 stands for the titrate volume; and B = weight (g) of the extract used.

Determination of vitamin E. The vitamin E content of HECP was quantified as previously described by Achikanu et al.²² The resulting solution's absorbance was measured at 520 nm against a blank, after which Equation 3 below was used to determine the quantity of vitamin E in the extract:

$$\text{Vitamin E (mg / 100 g)} = \frac{\text{AB of HECP} \times \text{Concentration. of standard}}{\text{AB of standard}} \quad (3)$$

where AB stands for absorbance.

Gas chromatography-flame ionization detector (GC-FID) phytochemical screening. Phytochemicals present in the extract were analysed by BUCK M910 gas chromatography coupled to a flame detector (GC-FID) according to the protocol described in Chukwuma et al¹ with the help of a RESTEK 15 m MXT-1 column (15 m x 250 µm x 0.15 µm). Phytochemicals were quantified using the internal standard's mass and area.

In vitro antioxidant assay

1,1-Diphenyl-2-picryl-hydroxyl radical-scavenging assay. The extract's ability to contribute the electron(s) necessary to convert 1,1-diphenyl-2-picryl-hydroxyl (DPPH) radicals (purple) to their hydrazine form (yellow) was examined using the protocol of Gyamfi et al.²³ The absorbance of serial dilutions of HECP (15.63-500 µg/mL) and ascorbic acid (the standard drug) was measured at 517 nm. After that, the scavenging of DPPH radicals was estimated using Equation 4.

$$\text{DPPH scavenging activity(\%)} = \frac{\text{AB of control} - \text{AB of HECP}}{\text{AB of control}} \times 100 \quad (4)$$

where AB stands for absorbance.

Ferric-reducing antioxidant power assay. The ferric-reducing antioxidant power assay (FRAP) of HECP was estimated by adopting the method of Oyaizu.²⁴ The absorbance of the Perl's Prussian blue complex, formed possibly after the reduction of Fe³⁺ to Fe²⁺, was spectrophotometrically measured at 700 nm. The FRAP activity was expressed as a gallic acid equivalent (GAE).

Inhibition of lipid peroxidation (TBARS) activity. The in vitro lipid peroxidation inhibitory effect of HECP was ascertained by measuring thiobarbituric acid-reactive substances (TBARS) following method of Banerjee et al²⁵ using butylated hydroxytoluene as the standard drug. In test tubes containing 100 µL of serially diluted solution of the sample (15.63-500 g/mL), 500 µL of rat brain homogenate was added, and the mixture was diluted

with distilled water to 1.0 mL. Following this, 50 μ L of 0.075 M FeSO_4 and 20 μ L of L-ascorbic acid were added, and the mixture was incubated for 60 minutes at 37°C. Subsequently, it was heated to 100°C for 15 minutes after adding 0.2 mL of EDTA (0.1 M) and 15 mL of TBA reagent. Finally, the test tubes were cooled and centrifuged, and the absorbance of the supernatant was measured at 532 nm. The lipid peroxidation inhibitory activity of the extract or standard was calculated with Equation 5.

$$\text{Lipid peroxidation inhibitory activity (\%)} = \frac{\text{AB of control} - \text{AB of HECP}}{\text{AB of control}} \times 100 \quad (5)$$

where AB stands for absorbance.

In vitro antidiabetic studies

Assay of α -amylase activity. The extract's ability to inhibit α -amylase activity was determined by the Kwon et al.²⁶ method using acarbose as a reference drug. The absorbance of varying concentrations of HECP and acarbose (100, 200, 300, and 500 μ g/mL) was measured at 540 nm. Subsequently, α -amylase activity was calculated using Equation 6.

$$\alpha\text{-amylase inhibitory activity (\%)} = \frac{\text{AB of control} - \text{AB of HECP}}{\text{AB of control}} \times 100 \quad (6)$$

Assay of α -glucosidase activity. The inhibitory effect of HECP on α -glucosidase activity was investigated using the experimental protocol of Matsui et al.²⁷ The amount of p-nitrophenyl formed after enzymatic dephosphorylation was determined by measuring the absorbance at 405 nm. The sample protocol was used for acarbose. The inhibition (%) was calculated as in Equation 7:

$$\alpha\text{-glucosidase inhibitory activity (\%)} = \frac{\text{AB of control} - \text{AB of HECP}}{\text{AB of control}} \times 100 \quad (7)$$

where AB stands for absorbance.

Crystal protein structure retrieval and preparation. The x-ray crystallography structures of human pancreatic amylase (5E0F) and alpha-glucosidase (3WY2) were retrieved from the Protein Data Bank (PDB). The proteins were prepared with the Schrodinger Suite v12.5 protein preparation wizard by assigning bond order and side chains, adding hydrogen, filling missing hoops, creating zero-order bond metals, deleting water beyond 5.00 Å, converting selenomethionine to methionine, assigning bond orders, simulated missing disulfide bonds, creating disulfide bonds, and removing water molecules beyond 5 Å. Finally, the restricted energy of the protein structure was minimized.

Preparation of ligands. The 3D structures of HECP phytochemical constituents determined by the GC-FID and those of the standard drug, acarbose, were obtained from PubChem (<https://pubchem.ncbi.nlm.nih.gov/>). The retrieved ligands were prepared with the Schrodinger Suite v12.5 LigPrep tools.

Prediction of binding sites and design of grid generation for molecular docking. The most favourable binding pockets and active catalytic sites of α -amylase (Site 1) and α -glucosidase (Site 2) were selected based on the predicted D score, site score, and volume (Supplementary Tables 1 and 2). In addition, using the grid construction tools of the Schrodinger Suite, the docking grid was created around the most probable binding site (Supplementary Figure 1).

Molecular docking and validation. The prepared ligands were docked into the enzymes' active sites as specified by the generated grid via extra-precision (XP) docking models on Schrodinger Suite v12.05. Subsequently, the 2D and 3D interactions of the hit compounds (chosen based on the X-glide score) were further investigated. The root mean square deviation (RMSD) value of the crystallographic structure pose of the co-crystallized ligand and the docked pose of α -glucosidase (3WY4) was also calculated to validate the docking programme (Supplementary Figure 2). The RMSD value of 0.6520 Å was obtained, which validates the accuracy of the docking software.²⁸

Pharmacology parameters. The canonical smiles of the identified compounds were assessed from the PubChem database (www.pubchem.com) and incorporated into the SwissADME web server (<http://www.swissadme.ch/>) to determine the ADME (adsorption, distribution, metabolism, and excretion) characteristics of the hit compounds. Physicochemical features not limited to molecular weight (MW), hydrogen bond donor and acceptor (HBD and HBA), n-octanol/water partition coefficient (Log P), number of rotatable bonds (Nrot), and topological polar surface area (TPSA) helped in predicting chemicals' drug-likeness in compliance with the rules of Egan et al.,²⁹ Veber et al.,³⁰ and Lipinski et al.³¹ Furthermore, gastrointestinal absorption, blood-brain barrier, P-glycoprotein inhibition/substrate, cytochrome P450 inhibition, and skin permeation were also estimated from SwissADME.

In addition, toxicity prediction such as LD₅₀, toxicity class, organ toxicity (hepatotoxicity), and toxicological effects, including mutagenicity, carcinogenicity, immunogenicity, and cytogeneticity, was estimated using the webserver of ProTox-II (https://tox-new.charite.de/protox_II).

Statistical analysis

The dataset generated from triplicate determinations of each experiment was analysed descriptively, deploying 1-way analysis of variance (ANOVA) and, subsequently, the Duncan post hoc analysis multiple comparisons test of IBM SPSS version

Table 1. Total phenols, total flavonoids, and vitamins composition of HECP.

COMPOUNDS	AMOUNTS
Phytochemicals	
Total phenols (mg/g GAE)	27.11 ± 0.61
Total flavonoids (mg/g QE)	8.49 ± 0.04
Vitamins (µg/g)	
Vitamin A	0.48 ± 0.01
Vitamin C	2.042 ± 0.41
Vitamin E	35.22 ± 3.14

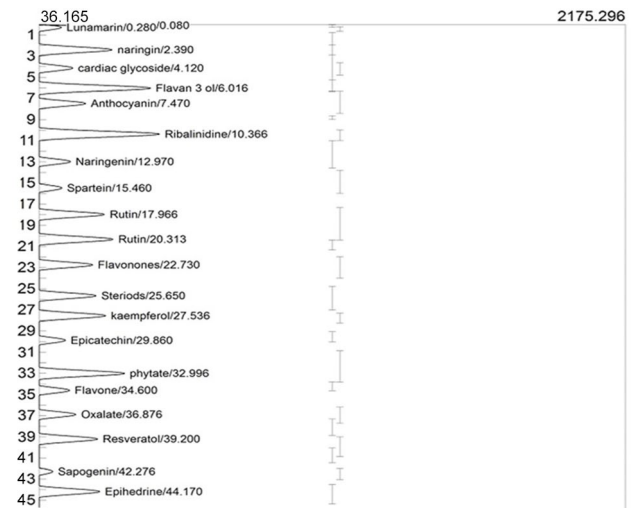
Values are recorded as mean ± SD of triplicate.

23 (SPSS Inc., Chicago, IL, USA). The mean ± SD of the results were presented, with $P < .05$ as a significant threshold. Furthermore, regression square (R²) and half maximal inhibitory concentration (IC₅₀) values were computed from the GraphPad Prism 6.5 software non-linear regression equation (GraphPad Software, Inc., California, USA).

Results and Discussion

Preliminary phytochemical screening and vitamin composition of HECP

Medicinal plants have recently become widely accepted and laudable due to their desired therapeutic effect on diabetic sufferers.^{5,32} Hydro-ethanolic extract of *C paniculatum* (HECP) is rich in phenols, flavonoids, and vitamin E, with moderate vitamin C and low vitamin A content (Table 1). Broadly speaking, phenols and flavonoids have demonstrated excellent antioxidant potential, the activity of which depends on the number and position of free OH groups in the phenolic ring.³³ Generally, the protective actions of flavonoids are attributed to their free radical neutralizing effect, oxidase inhibition, and capacity to activate antioxidant enzymes.^{34,35} Ideally, as oxidative stress is intrinsically implicated in diabetes onset and progression, flavonoids could immensely benefit patients with diabetes. Flavonoids improve oxidative metabolism, derange glucose levels, and stimulate insulin secretion in the diabetic state by altering the intracellular concentrations of Ca²⁺.³⁶ Previous studies reported a linear correlation between total phenols, flavonoids, and antioxidant activity. Also, dietary intake of vitamins improves pancreatic β-cell function, which prevents or delays the transition from pre-diabetes to DM. According to Chukwuma et al,¹ vitamin A enhances pancreatic function, β-cell regeneration, insulin sensitivity, and secretion via activation of glucokinase promoters, increasing pancreatic glucokinase, which mitigates insulin resistance. Emerging data have revealed that vitamin E, usually deficient in patients with diabetes, is a chain-breaking antioxidant known to improve insulin sensitivity and metabolic control in diabetes.³⁷ The

**Figure 1.** GC-FID chromatogram of compounds present in HECP.

interaction of vitamin E with the cysteine residues of protein kinase C prevents the overproduction of ROS. Hence, vitamin E-enriched agents hold great appeal in DM treatment because they mitigate downstream signalling responsible for insulin resistance, impaired insulin secretion, and the induction of diabetic complications.³⁸

GC-FID phytochemical profiling of HECP

Some essential phytochemicals with well-established biological properties were identified in HECP using GC-FID. Among these, flavonoids (proanthocyanidin, naringin, flavan-3-ol, anthocyanin, naringenin, rutin, flavanones, kaempferol, epicatechin, flavone, and resveratrol) were found to be the major compounds. Other compounds also identified were glycosides (linamarin), steroids (cardiac glycoside and steroids), alkaloids (ribalinidine, sparteine, and ephedrine), and anti-nutrients (phytate and oxalate) (Figure 1 and Table 2). Proanthocyanidin and anthocyanin, which contain the glycosyl and aglycone groups, serve as stress protectants in plants and have health-promoting effects due to their potent antioxidant, inflammatory, and blood glucose-regulating actions.^{34,39} Anthocyanidins exert antidiabetic activity mainly by inhibiting oxidative stress, promoting insulin secretion, and improving insulin resistance.³⁹ To lend credence to this statement, Johnson and de Mejia⁴⁰ recorded increased insulin secretion and regulated Dipeptidyl peptidase IV (DPPIV). They upregulated mRNA expression in insulin receptor-related genes after anthocyanidin supplementation. Moreover, Egbuna et al⁴¹ reported that anthocyanins protected against β-cell injury and autophagy mediated by H₂O₂ by upregulating the expression of HO-1 and transcription factor Nrf2 and also improved glucose tolerance, serum insulin level, and restored blood glucose in Streptozotocin-induced diabetic rats. Naringenin's pharmaceutical activities include antioxidant, anti-inflammatory, antidepressant, anti-hyperlipidaemia, and

Table 2. Phytochemicals identified in hydro-ethanolic extract of *C paniculatum* using GC-FID.

PEAK NO	IDENTIFIED COMPOUNDS	RETENTION TIME (MINUTES)	PEAK AREA	PEAK HEIGHT	CONC. (µG/G)	CLASS OF COMPOUNDS
1	Proanthocyanidin	0.080	232.8066	139.940	0.2183	Flavonoid
2	Lunamarin	0.280	3400.3980	117.455	4.9786	Glycoside
3	Naringin	2.390	12252.8106	301.042	15.2487	Flavonoid
4	Cardiac glycoside	4.120	6344.5478	157.568	3.9370	Steroid
5	Flavan-3-ol	6.016	18154.0688	442.689	10.5455	Flavonoid
6	Anthocyanin	7.470	8442.9838	206.428	7.2410	Flavonoid
7	Ribalinidine	10.366	19598.0668	476.646	8.4040	Alkaloid
8	Naringenin	12.970	6238.3258	152.341	2.6361	Flavonoid
9	Sparteine	15.460	4967.5639	121.273	8.9024	Alkaloid
10	Rutin	17.966	11339.2568	276.424	7.0365	Flavonoid
11	Rutin	20.313	12756.4840	307.630	7.9159	Flavonoid
12	Flavanones	22.730	9573.1408	233.186	8.2102	Flavonoid
13	Steroids	25.650	10008.8176	245.115	17.1678	Steroid
14	Kaempferol	27.536	11458.0104	280.295	5.2899	Flavonoid
15	Epicatechin	29.860	5478.4406	133.723	8.2188	Flavonoid
16	Phytate	32.996	14009.1853	345.703	18.8296	Anti-nutrient
17	Flavone	34.600	5756.4320	144.579	3.5721	Flavonoid
18	Oxalate	36.876	6988.5601	170.310	11.0380	Anti-nutrient
19	Resveratrol	39.200	10234.6024	249.263	7.7771	Flavonoid
20	Sapogenin	42.276	3473.1416	85.310	5.7077	Saponin
21	Ephedrine	44.170	10509.6768	256.782	13.5202	Alkaloid

antidiabetic properties.³⁴ Naringenin plays an essential role in DM, where it regulates hyperglycaemia by inhibiting the reabsorption of glucose in the renal tubule and the intestinal brush border, as well as increasing glucose uptake and utilization by muscle and fat tissues.¹ Similarly, rutin and kaempferol help control hyperglycaemia by increasing insulin secretion and release, increasing glucose uptake in peripheral tissues, and stopping gluconeogenesis.⁴¹ Studies have shown that epicatechin consumption reduces hyperglycaemia in patients with diabetes. Moreover, resveratrol is a dietary stilbene known to modulate the inflammatory response, reduce oxidative stress, and protect the pancreatic β -cell. Restoring the activities of enzymes involved in glucose homeostasis altered in diabetic individuals, reversing the degeneration of beta cells, and inhibiting beta cell apoptosis via the inhibition of caspase-3 are the critical mechanisms of the antidiabetic actions of resveratrol.³⁹ It is worth noting that several animal, cell, and clinical studies have convincingly confirmed the antidiabetic activity

of resveratrol.^{39,41} Ribalinidine, sparteine, and ephedrine are quinoline alkaloids pharmacologically active as radical scavengers.⁴² Intriguingly, the availability of these antidiabetic compounds in *C paniculatum* leaves could account for its high therapeutic efficacy.

In vitro antioxidant activities of HECP

Oxidative stress is linked to the pathophysiology of DM because of its consequences or as a causative agent.¹ Under sustained hyperglycaemia, ROS build up because of glucose autooxidation, non-enzymatic glycation, and a drop in glutathione levels. This leads to cell dysfunctions, insulin resistance, and diabetic vascular complications.^{38,43} Hence, several clinical trials targeting ROS sources are ongoing as possible targets for treating diabetes and its complications.³⁸ Within the frame of this study, HECP demonstrated good DPPH, TBARS, and FRAP inhibitory effects, which were maximal at

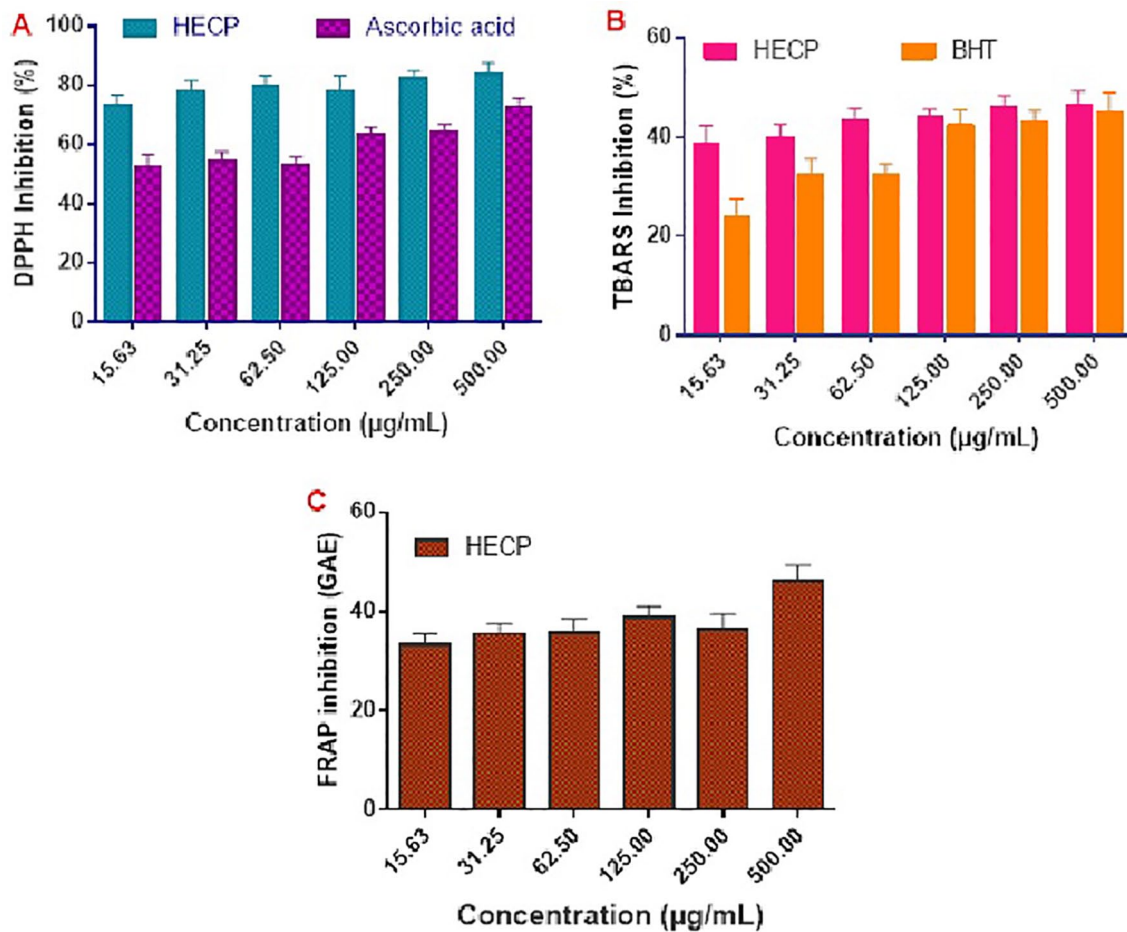


Figure 2. Antioxidant activity of the extract and standards determined by (A) DPPH radical scavenging activity, (B) TBARS inhibition and (C) FRAP. Results are presented as mean \pm SD of determinations made in three replicates.

500 $\mu\text{g/mL}$ (Figure 2). Comparatively, the DPPH (IC_{50} value 0.8254 $\mu\text{g/mL}$) and TBARS (IC_{50} value 2.284 $\mu\text{g/mL}$) inhibitory capacities of the extract were higher than the 4.452 and 13.16 $\mu\text{g/mL}$ recorded in the standards, ascorbic acid, and butylated hydroxytoluene, respectively (Figure 3). The ability of the extract to reduce the DPPH radical (purple) to the stable hydrazine form (light yellow) and Fe^{3+} to Fe^{2+} in the FRAP assay shows its potential as a laudable antioxidant agent.

Furthermore, inhibition of malondialdehyde formation in the TBARS assay further highlights the extract's antioxidant properties and suggests its potential to prevent peroxidation of the biomembranes. The identified bioactive compounds, including vitamins and phytochemicals, could be responsible for the antioxidant action.⁴⁴ In general, polyphenols identified in the extract donate electrons from their multiple phenolic rings to scavenge free radicals, with subsequent stabilization due to the resonance structure of the phenolic ring. These findings provide insight into HECP's ability to scavenge the excessive free radicals and other oxidant species generated under diabetic conditions. This will avert oxidative stress-mediated complications in patients with DM. Earlier studies have shown

that modulating oxidative stress, which is the central mediator of autoimmune destruction of beta cells in T1D or malfunction of beta cells, glucotoxicity, and insulin resistance in T2D, will not only help in regulating glucose levels but will also prevent the onset of diabetes.⁴³ As a result, the exciting antioxidant capacity of HECP makes it a valuable agent for antidiabetic drug discovery.

In vitro antidiabetic activities of HECP

Increasing evidence has shown that controlling postprandial glucose levels is a crucial and practical approach to preventing DM in high-risk and pre-diabetic individuals.^{1,14,36,45} Interestingly, HECP demonstrated potent inhibitory properties against α -amylase and α -glucosidase in a concentration-dependent manner, with IC_{50} values of 14.21 and 13.23 $\mu\text{g/mL}$, respectively. These values were found to be comparable with 13.06 $\mu\text{g/mL}$ (α -amylase) and 11.71 $\mu\text{g/mL}$ (α -glucosidase) inhibitory effects recorded with the standard drug, acarbose (Figures 4 and 5). Accordingly, inhibition of α -amylase needed to break α (1 \rightarrow 4) glycosidic linkages of

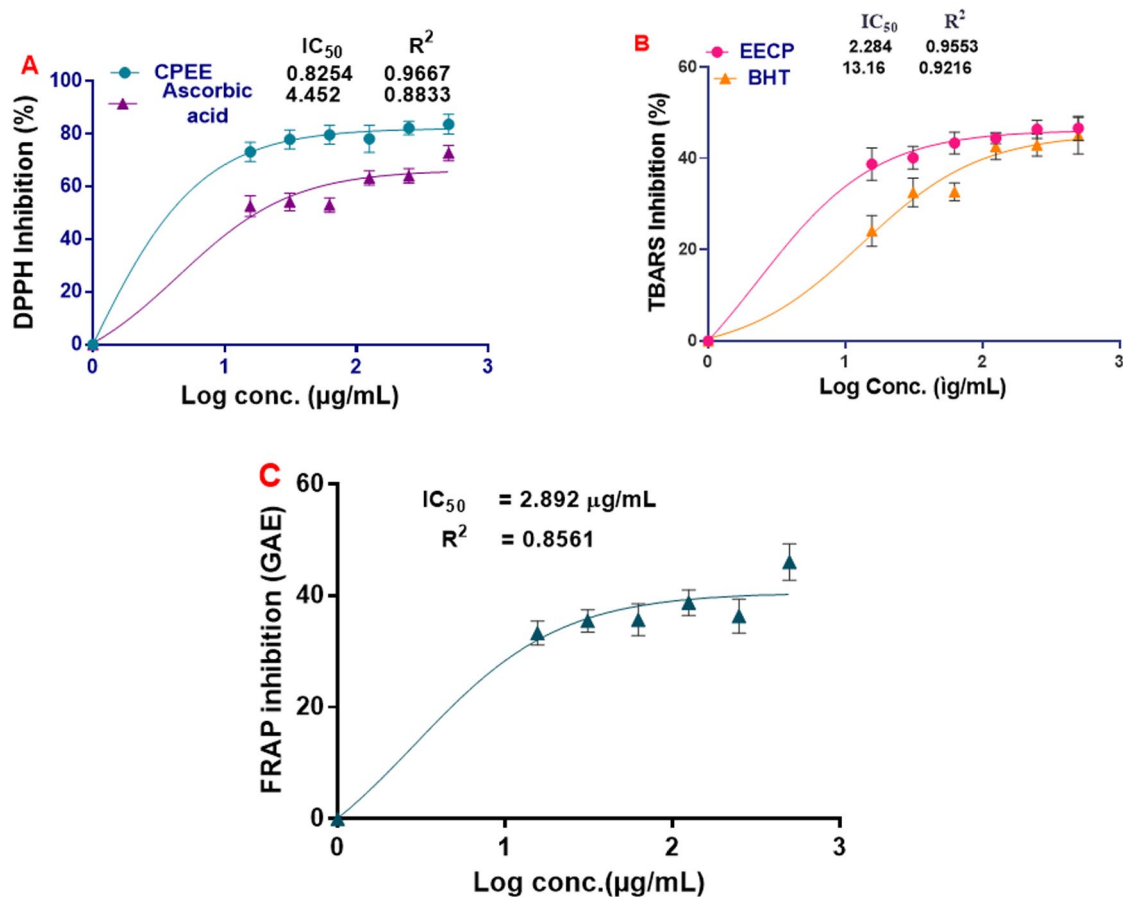


Figure 3. Non-linear regression curve for IC_{50} and regression values of DPPH (A), TBARS (B) and FRAP (C) inhibitory activities of the extract and standard drugs. Results are presented as mean \pm SD of determinations made in three replicates.

carbohydrates and starch to oligosaccharides and α -glucosidase, which regulates glucose absorption in the small intestine, is a pointer to the antidiabetic action of the extract. Ideally, α -amylase inhibitors prevent the absorption of dietary starch, which has beneficial effects on insulin resistance and glycaemic index control in people with diabetes.⁴⁶ In addition, inhibition of α -glucosidase has a remarkable impact on polysaccharide metabolism and cellular interaction, opening up new avenues for drugs targeting diabetes, metastatic cancer, and viral infection.⁴⁷ As previously reported, regulation of these enzymes controls postprandial hyperglycaemia, decreases glycated haemoglobin levels, and averts diabetic complications in patients.³⁷ The synergic effects between the polyphenols and other bioactive compounds present in HECP on the carbohydrate-binding regions of these enzymes could be responsible for the observed effects. Indeed, flavonoids, vitamin E, and alkaloids present in high amounts in the extract have demonstrated antidiabetic actions in several studies. These results are in tandem with previous studies by Miaffo et al⁴⁸ and Chika and Bello,⁴⁹ who reported α -amylase and α -glucosidase inhibitory effects

of *Combretum molle* twigs and antihyperglycaemic activity of *Combretum micranthum* in alloxan-induced diabetic rats, respectively.

In silico antidiabetic compounds identified from HECP

Molecular docking is a valuable asset used in drug discovery and development to model interactions between potential drug candidates and receptors or proteins implicated in the etiopathogenesis of diseases due to its high precision.^{14,50,51} We evaluated the molecular interactions of the bioactive compounds from HECP with α -amylase and α -glucosidase. Hydro-ethanolic extract of *C paniculatum* phytoligands interacted favourably in the binding domain of α -amylase, with rutin having the best binding score of -11.307 kcal/mol. Other top-scoring ligands, kaempferol, epicatechin, ephedrine, and resveratrol, had docking scores of -7.797 , -6.652 , -6.289 , and -6.206 kcal/mol, respectively (Table 3). Understanding the type and number of interactions between protein-ligand complexes provides vital

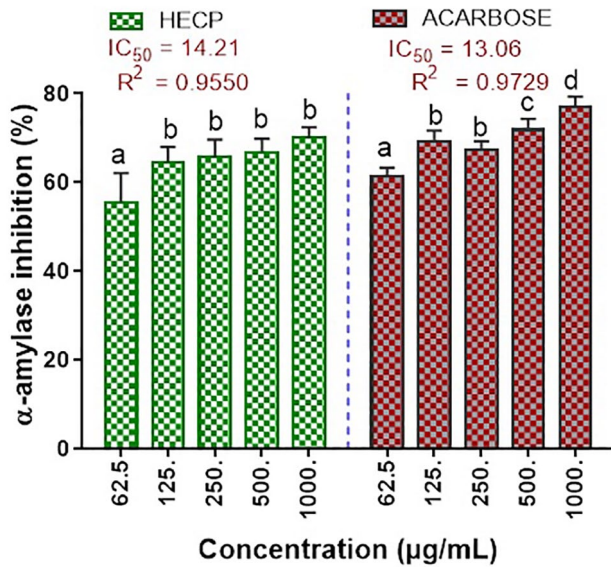


Figure 4. Inhibitory effects of HECP on α -amylase activity. Results are presented as Mean \pm SD (n=3). A sample's percentage inhibition with different alphabet is statistically significant at $p < 0.05$. However, mean values with the same alphabetic letters do not differ significantly ($p > 0.05$).

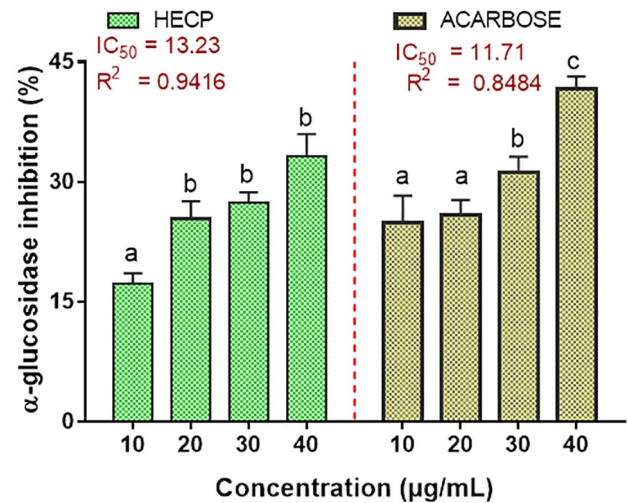


Figure 5. Inhibitory effect of HECP on α -glucosidase activity. Results are presented as Mean \pm SD (n=3). A sample's percentage inhibition with different alphabet is statistically significant at $p < 0.05$. However, mean values with the same alphabetic letters do not differ significantly ($p > 0.05$).

Table 3. Top-scoring compounds from HECP and their molecular interactions with α -amylase and α -glucosidase.

COMPOUNDS	PUBCHEM CID	DOCKING SCORES (KCAL/MOL)	XP GSCORE (KCAL/MOL)	NO H-BONDS	INTERACTING AMINO ACID RESIDUES
α-amylase					
Rutin	5280805	-11.307	-11.307	6	^h TRP59, ^h ASP356, ^h HIP305, ^h ASP197, ^h GLU223, ^h HIP305, [#] TRP59, [#] HIP305
Kaempferol	5280863	-7.797	-7.797	2	^h TYR59, ^h GLU233, [#] HIS201
Epicatechin	72276	-6.652	-6.652	3	^h ASP197, ^h GLN63, [#] TYR62, [#] TRP59
Ephedrine	9294	-6.289	-6.252	1	^h ASP197, [*] GLU233
Resveratrol	445154	-6.206	-6.206	4	^h THR163, ^h TRP59, ^h GLN63, ^h GLU233, [#] TYR62
Acarbose	41774	-11.542		6	^h GLN63, ^h TRP59, ^h ASP197, ^h HIS201, ^h LYS200, ^h THR163, ^h GLU240
α-glucosidase					
Epicatechin	72276	-8.963	-8.963	4	^h ARG400, ^h ASP62, ^h HIE105, ^h GLY228, [#] PHE296
Kaempferol	5280863	-8.359	-8.391	4	^h AST202, ^h HIE105, ^h ASP333, ^h GLY273, [#] TYR65
Naringenin	439246	-8.177	-8.195	4	^h GLY273, ^h ARG400, ^h ASP202, ^h HIE105, [#] TYR65
Ephedrine	9294	-8.174	-8.181	3	^h ASP202, ^h ARG400, ^h ASP62, [*] PHE166, ^{π} ASP202
Resveratrol	445154	-8.102	-8.102	3	^h ASP62, ^h HIE332, ^h ASP202, [#] TYR65
Acarbose	41774	-7.194	-7.332	3	^h LYS467, ^h GLU439, ^h GLU532

^hH-bond, [#] π - π stacking, ^{*}Pi-cation, and ^{π} salt bridge.

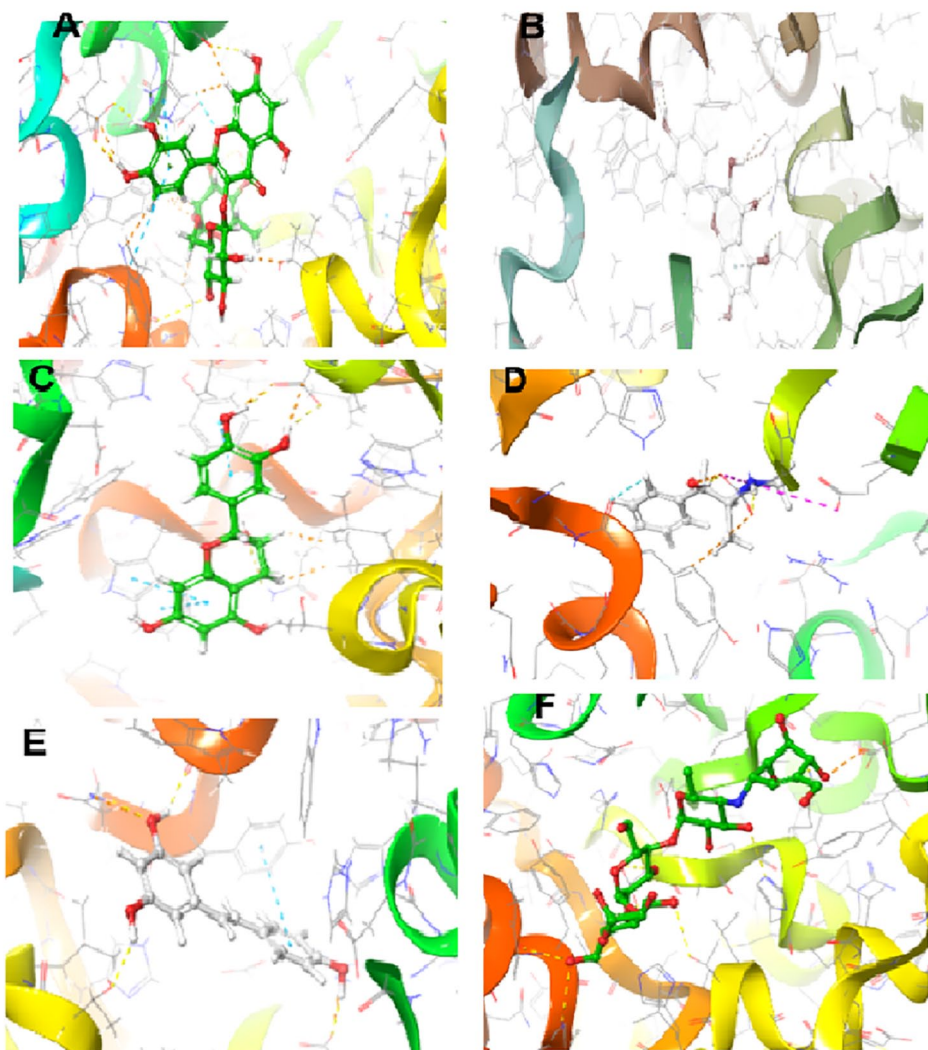


Figure 6. Three dimensional (3D) representation of the ligand-receptor complex formed between α -amylase and the hits compounds: A= rutin, B = Kaempferol, C = epicatechin, D = Ephedrine, E = Resveratrol and H = Acarbose.

information on the mechanisms of action of the latter ligands against DM.⁵ Interestingly, hydrogen bonding, pi-pi stacking, and pi-cation interactions between our top-scoring compounds and the active site amino acid residues of α -amylase indicate the formation of well-established complex stability. As revealed from enzyme kinetics and x-ray crystallographic studies, the α -amylase active site contains ASP197, ASP300, and GLU233 amino acid residues.^{1,2,37} In the hydrolysis of starch, ASP 197 is a catalytic nucleophile; ASP 300 helps optimize the substrate orientation; and GLU 233 acts as an acid-base catalyst.³⁷ Furthermore, rutin and epicatechin formed H-bonds with ASP197 using hydroxyl groups found in their phenolic rings. Similarly, resveratrol had hydrogen bonding with GLU233, while ephedrine had pi-cation interactions with GLU233 and hydrogen bonding with ASP197 (Figures 6 and 7 and Table 3).

It is worth mentioning that interactions with ASP197 and GLU233 present in the α -amylase active site domain will cause strong geometric constraints, thereby inhibiting the subsequent binding of substrate (starch) from releasing glucose.³⁷ In addition, high-binding affinity with docking scores in the range of -8.102 to -8.963 kcal/mol was recorded between our ligands and α -glucosidase. This was comparatively higher than the -7.194 kcal/mol registered with acarbose. The interactions of the top-scoring compounds with α -glucosidase were mainly mediated by conventional H-bonds, pi-cation, pi-pi stacking, salt bridge formation around the active site, and catalytic amino acid residues (Figures 8 and 9). Collectively, the high docking scores exhibited by HCEP compounds with α -amylase and α -glucosidase denote their therapeutic efficacy against DM.

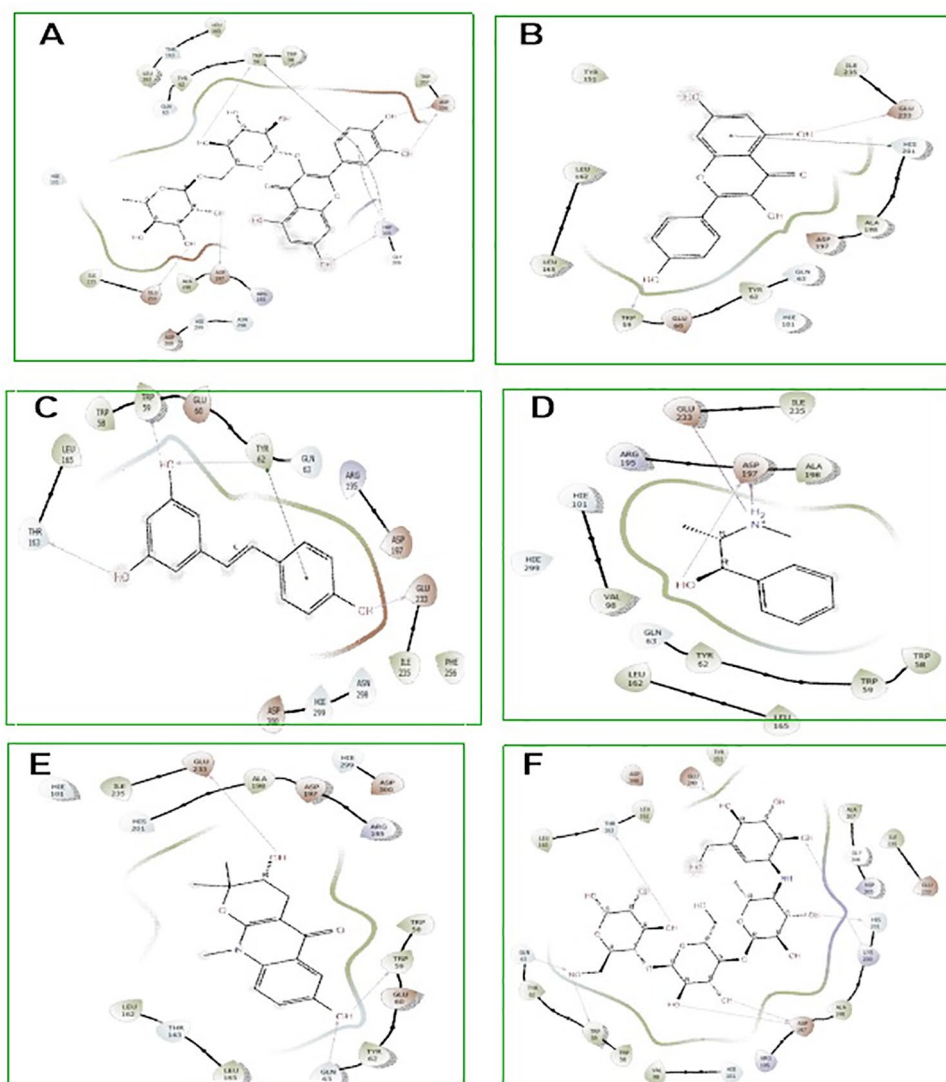


Figure 7. Two dimensional (2D) representation of molecular docking poses of best hit compounds from the HECF with amylase. A= rutin, B =Kaempferol, C= epicatechin, D= Ephedrine, E= Resveratrol and H =Acarbose.

ADMET properties of the top-scoring compounds

Conventionally, *in silico* prediction of absorption–distribution–metabolism–excretion–toxicity (ADMET) properties is crucial in ascertaining pharmacological efficacy and safety, which are major decisive factors that lead to drug failure in clinical trials.^{37,52} It determines if a compound is orally absorbable, well distributed to its specific target, swiftly metabolized, and quickly eliminated without provoking adverse effects in the body.⁵³ The zero violation of the drug-likeness rules of Lipinski, Veber, and Egan by the hit compounds revealed that they are good oral drugs, as also corroborated by their 0.55% bioavailability scores (Table 4). Drug candidates that obey Lipinski, Veber, and Egan rules have a high chance of becoming marketable due to their lower attrition rate when subjected to clinical trials.^{6,44} Furthermore, the hit compounds had good

pharmacokinetics and toxicity profiles, as shown in Table 5. The hits' high gastrointestinal absorption (GIA) potentials make them an optimal therapeutic agent for reducing the activities of α -glucosidase and subsequent glucose absorption in the intestinal brush border. At the same time, the non-inhibition of all the CYP 450 isoforms by rutin, epicatechin, and ephedrine suggests that they could be easily biotransformed to water-soluble compounds easily eliminated in the urine to reduce organ toxicity due to interaction with other drugs.⁵⁴ The CYP 450 family, particularly isoforms 1A2, 2C9, 2C19, 2D6, and 3A4, is responsible for about 90% of oxidative metabolic reactions.⁵⁵ According to Apeh et al,⁵⁶ inhibition of more CYP isoforms by a given molecule shows that it has the potential to have drug-drug interactions with other drugs. Most importantly, the toxicity results of the hit compounds show that they are safe, as revealed by their LD₅₀ values in the range

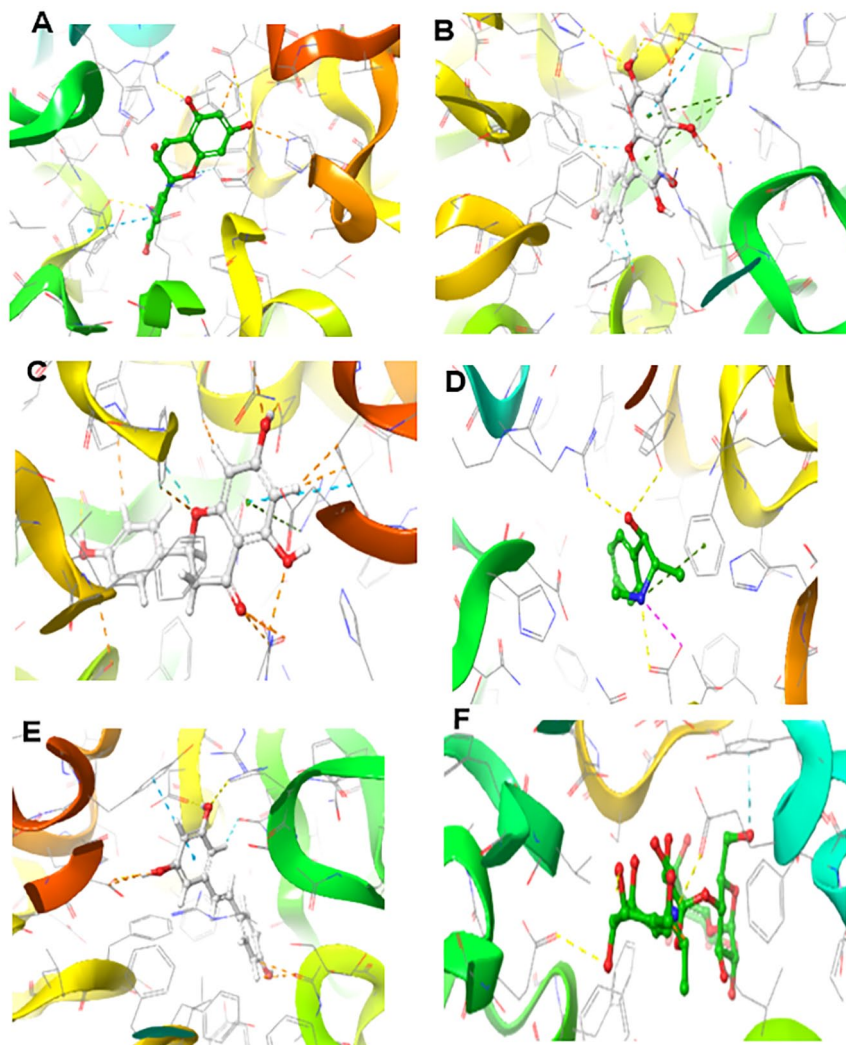


Figure 8. Three dimensional (3D) representation of the ligand-receptor complex formed between α -glucosidase and the hits compounds: A= Epicatechin, B =Kaempferol, C=, Naringinin D= Ephedrine, E= Resveratrol and H =Acarbose.

of 404 to 10.000 kg/b.w. It is also worth mentioning that they belong to safe toxicity classes 4 to 6 and are not likely to be hepatotoxic or carcinogenic.

Conclusions

This research indicates that the hydro-ethanolic extract of *C paniculatum* possesses profound potential as an antioxidant and antidiabetic agent, as revealed from the in vitro experiments.

Furthermore, 7 GC-FID-identified compounds established satisfactory results as promising inhibitors of α -amylase and α -glucosidase in our in silico experiments. It is, therefore, expedient to conclude that the extract's rich bioactive compounds might be responsible for the antidiabetic activity. Thus, the extract contains lead phytochemicals, which could serve as therapeutics for developing novel antidiabetic drugs. However, this could be further substantiated using in vivo experiments.

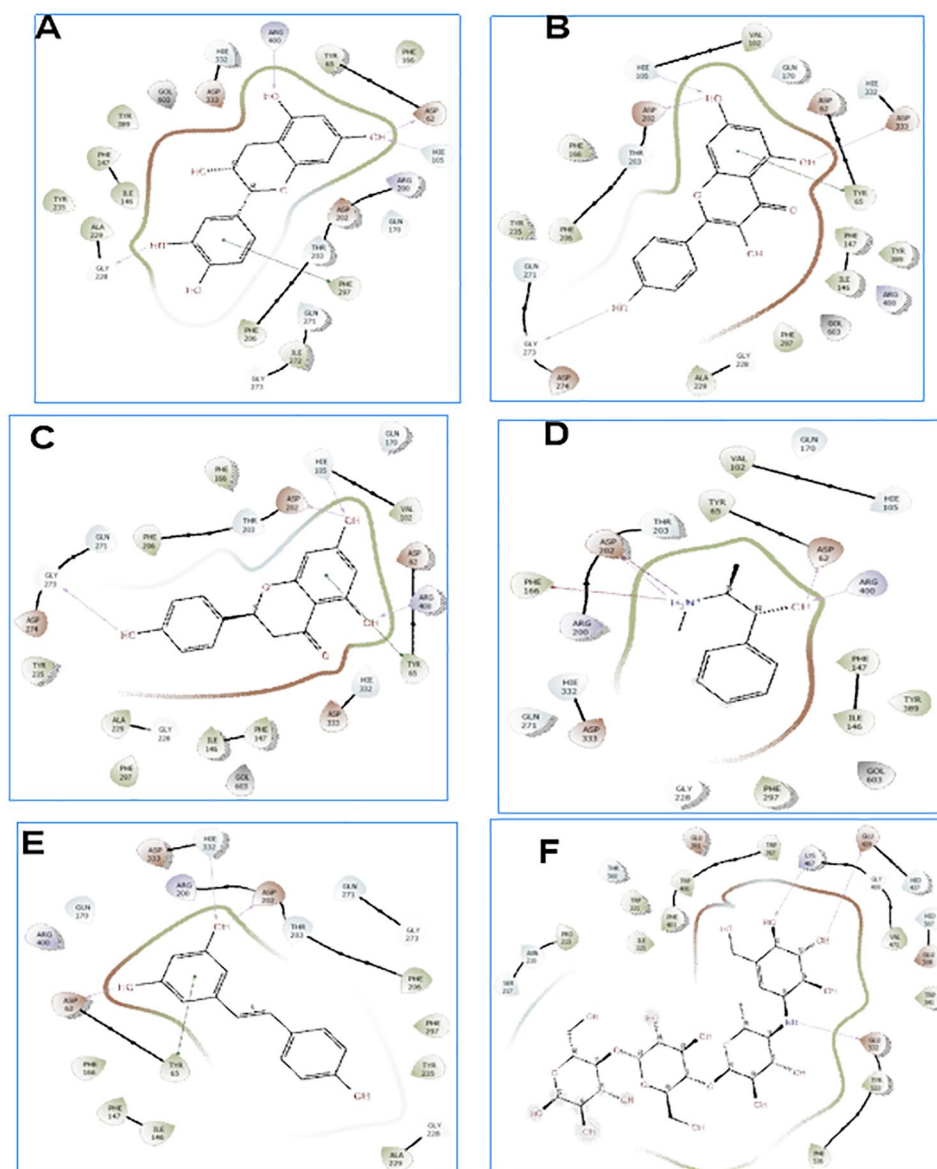


Figure 9. Two dimensional (3D) representation of the ligand-receptor complex formed between α -glucosidase and the hits compounds: A= Epicatechin, B=Kaempferol, C=, Naringenin D= Ephedrine, E= Resveratrol and H =Acarbose.

Table 4. Predicted drug-likeness of the top-scoring compounds identified from HECP.

COMPOUNDS	MW (G/MOL)	LOG P	#HBA	# HBD	NROT	TPSA	BAS	NO. OF VIOLATIONS		
								LIPINSKI	VEBER	EGAN
Rutin	610.52	2.43	16	10	6	269.43	0.17	3	1	1
Kaempferol	286	1.7	6	4	1	111.1	0.55	0	0	0
Epicatechin	290	1.47	6	5	1	110.4	0.55	0	0	0
Ephedrine	165.23	2.25	2	2	3	32.26	0.55	0	0	0
Naringenin	272	1.75	5	3	1	86.99	0.55	0	0	0
Resveratrol	228	1.71	3	3	2	60.69	0.55	0	0	0
Acarbose	645.6	0.63	19	14	9	321.17	0.17	3	1	1

Values in red and green colours are above the reference range of drug-like compounds.

Abbreviations: MW, molecular weight (g/mol); Log P, octanol-water partition coefficient; HBA, hydrogen bond acceptor; HBD, hydrogen bond donor; TPSA, topological polar surface area; Nrot, # rotatable hydrogen bond; BAS, bioavailability score.

Table 5. Pharmacokinetics and toxicity prediction output of HECF compounds.

PROPERTIES	A	B	C	D	E	F	G
Pharmacokinetics							
GIA	Low	High	High	High	High	High	Low
BBB	No	No	No	Yes	No	Yes	No
P-gp substrate	Yes	No	Yes	No	Yes	No	Yes
CYP1A2	No	Yes	No	No	No	Yes	No
CYP2C19	No	No	No	No	No	No	No
CYP2C9	No	No	No	No	No	Yes	No
CYP2D6	No	Yes	No	No	No	No	No
CYP3A4	No	Yes	No	No	Yes	Yes	No
Log kp (cm/s)	-10.26	-6.7	-7.82	-6.65	-6.2	-5.47	-16.29
Toxicity							
LD ₅₀ (mg/kg)	5000	3919	10 000	404	2000	1560	24 000
Toxicity class	5	5	6	4	4	4	6
Hepatotoxicity	Inactive	Inactive	Inactive	Inactive	Inactive	Inactive	Active
Carcinogenicity	Inactive	Inactive	Inactive	Inactive	Inactive	Inactive	Inactive
Immunogenicity	Active	Inactive	Inactive	Inactive	Inactive	Inactive	Active
Mutagenicity	Inactive	Inactive	Inactive	Inactive	Inactive	Inactive	Inactive
Cytotoxicity	Inactive	Inactive	Inactive	Inactive	Active	Inactive	Inactive

Abbreviations: A=rutin, B=Kaempferol, C=epicatechin, D=Ephedrine, E=Naringinin, F=Resveratrol, and H=acarbose.

Author Contributions

Ifema F Chukwuma: Conceptualization, Methodology, Investigation, Data curation, Software, supervision, Writing - critical review and editing; **Chidi E Atikpoh, Florence N Nworah, and Victor O Apeh:** Investigation, Data analysis, Writing - original draft. **Lawrence US Ezeanyika:** Methodology, Investigation, Formal analysis, Supervision, Writing - critical review and editing.

DATA AVAILABILITY STATEMENT

The data set generated in this research is contained within the article or in the supplementary material.

ORCID iDs

Chidi E Atikpoh  <https://orcid.org/0009-0006-5792-9365>

Victor O Apeh  <https://orcid.org/0000-0003-2987-4046>

SUPPLEMENTAL MATERIAL

Supplemental material for this article is available online.

REFERENCES

1. Chukwuma IF, Nworah FN, Apeh VO, et al. Phytochemical characterization, functional nutrition, and anti-diabetic potentials of *Leptadenia bastata* (pers) Decne Leaves: in silico and in vitro studies. *Bioinform Biol Insights*. 2022;16:11779322221115436. doi:10.1177/11779322221115436
2. Onikanni AS, Lawal B, Olusola AO, et al. *Sterculia tragacantha* lindl leaf extract ameliorates STZ-induced diabetes, oxidative stress, inflammation and neuronal impairment. *J Inflamm Res*. 2021;14:6749-6764. doi:10.2147/JIR.S319673
3. Burgos-moron E, Abad-jim Z, Marañon AM, et al. Relationship between oxidative stress, ER stress, and inflammation in type 2 diabetes: the battle continues. *J Clin Med*. 2019;8:1385-1406.
4. Alam S, Sarker MMR, Sultana TN, et al. Antidiabetic phytochemicals from medicinal plants: prospective candidates for new drug discovery and development. *Front Endocrinol*. 2022;13:800714. doi:10.3389/fendo.2022.800714
5. Rampadarath A, Balogun FO, Sabiu S. Insights into the mechanism of action of *Helianthus annuus* (sunflower) seed essential oil in the management of Type-2 diabetes mellitus using network pharmacology and molecular docking approaches. *Endocrines*. 2023;4:327-349.
6. Kikiowo B, Ogunleye JA, Iwaloye O, Ijatuyi TT. Therapeutic potential of *Chromolaena odorata* phyto-constituents against human pancreatic α -amylase. *J Biomol Struct Dyn*. 2022;40:1801-1812. doi:10.1080/07391102.2020.1833758
7. Chukwuma IF, Apeh VO, Chiletugo OF. Mechanisms and potential therapeutic targets of hyperinflammatory responses in SARS-CoV-2. *Acta Virol*. 2021;65:3-9. doi:10.4149/av_2021_102
8. Pasupuleti VR, Arigela CS, Gan SH, et al. A review on oxidative stress, diabetic complications, and the roles of honey polyphenols. *Oxid Med Cell Longev*. 2020;2020:8878172. doi:10.1155/2020/8878172
9. Migheli R, Lostia G, Galleri G, et al. New perspective for an old drug: can naloxone be considered an antioxidant agent? *Biochem Biophys Res*. 2023;34:101441. doi:10.1016/j.bbrep.2023.101441

10. Iacobini C, Vitale M, Pesce C, Pugliese G, Menini S. Diabetic complications and oxidative stress: a 20-year voyage back in time and back to the future. *Anti-oxidants*. 2021;10:727-749. doi:10.3390/antiox10050727
11. Darenkaya MA, Kolesnikova LI, Kolesnikov SI. Oxidative stress: pathogenetic role in diabetes mellitus and its complications and therapeutic approaches to correction. *Bull Exp Biol Med*. 2021;171:179-189. doi:10.1007/s10517-021-05191-7
12. Ratnaningtyas NI, Hernayanti H, Ekowati N. Ethanol extract of the mushroom *Coprinus comatus* exhibits antidiabetic and antioxidant activities in streptozotocin-induced diabetic rats antioxidant activities in streptozotocin-induced diabetic rats. *Pharm Biol*. 2022;60:1126-1136. doi:10.1080/13880209.2022.2074054
13. Xiao Q, Wang L, Supekar S, et al. Structure of human steroid 5 α -reductase 2 with the anti-androgen drug finasteride. *Nat Commun*. 2020;11:5430. doi:10.1038/s41467-020-19249-z
14. Shah S, Talukder SH, Uddin AMK, et al. Comparative assessment of three medicinal plants against diabetes and oxidative stress using experimental and computational approaches. *Evidence-based Complement Altern Med*. 2023;2023:635981815. doi:10.1155/2023/6359818
15. Nkwocha CC, Ogugofor MO, Chukwuma IF, Njoku OU. Identification and characterization of phytochemicals and constituents in *Desmodium velutinum* stem using high-performance liquid chromatography (HPLC). *Pharmacol Res Mod Chinese Med*. 2022;3:100090. doi:10.1016/j.prmcm.2022.100090
16. Chukwuma IF, Apeh VO, Nworah FN, Nkwocha CC, Mba SE, Ossai EC. Phytochemical profiling and antioxidative potential of phenolic-rich extract of *Cola acuminata* nuts. *Biointerface Res Appl Chem*. 2023;13:29-39. doi:10.33263/BRIAC131.029
17. Chukwuma IF, Aniagboso KT, Atrogo BE, et al. Elucidation of the phytochemicals, safety profile, and preclinical anti-inflammatory activity of ethanol extract of *Combretum paniculatum* leaves. *Trop J Nat Prod Res*. 2022;6:2035-2040.
18. Ogundajo AL, Kazeem MI, Evroh JE, Avoseh MM, Ogunwande IA. Comparative study on the phytochemical compositions and antihyperglycemic potentials of the leaves extracts of *Combretum paniculatum* and *Morinda morindoides* comparative study on the phytochemical compositions and antihyperglycemic potentials of the leaves. *European J Med Plants*. 2015;7:77-86. doi:10.9734/EJMP/2015/15929
19. Singleton VL, Rossi JA. Colorimetric of total phenolics with phosphomolybdic-phosphotungstic acid reagents. *Am J Enol Vinic*. 1965;16:144-158.
20. Zhishen J, Mengcheng T, Jianming W. The determination of flavonoid contents in mulberry and their scavenging effects on superoxide radicals. *Food Chem*. 1999;64:555-559. doi:10.1016/S0308-8146(98)00102-2
21. AOAC. *Official Methods of Analysis*. 19th ed. Washington, DC: Association of Official Analytical Chemist; 2012
22. Achikanu CE, Ude CM, Ugwuokolie OC. Determination of the vitamin and mineral composition of common leafy vegetables in south eastern Nigeria. *Int J Curr Microbiol App Sci*. 2013;2:347-353.
23. Gyamfi MA, Yonamine M, Aniya Y. Free radical scavenging action of medical herbs from Ghana: *Ibboningia sanguinea* on experimentally induced liver injuries. *Gen Pharmacol*. 1999;32:661-667.
24. Oyazui M. Studies on products of browning reactions: antioxidant activities of products of browning reaction prepared from glucosamine. *JPN J Nutr*. 1986;44:307-315.
25. Banerjee A, Dasgupta N, De B. In vitro study of antioxidant activity of *Syzygium cumini* fruit. *Food Chem*. 2005;90:727-733. doi:10.1016/j.foodchem.2004.04.033
26. Kwon Y, Apostolidis E, Shetty K. α -amylase and α -glucosidase for management of hyperglycemia linked to type 2 diabetes. *J Food Biochem*. 2008;32:15-31.
27. Matsui T, Yoshimoto C, Osajima K, Oki T, Osajima Y. In vitro survey of α -glucosidase inhibitory food components. *Biosci Biotechnol Biochem*. 1996;60:2019-2022.
28. El-Kelawy HM, Mansour MA, El-Naggar RE, Nabila E, Elkassas E. Effect of garlic (*Allium sativum*) treatment on hematological, biochemical, hormonal and fertility parameters of male bouscat rabbits. *Egypt J Rabbit Sci*. 2017;27:341-358.
29. Egan WJ, Merz KM, Baldwin JJ. Prediction of drug absorption using multivariate statistics. *J Med Chem*. 2000;43:3867-3877. doi:10.1021/jm000292e
30. Veber DF, Johnson SR, Cheng HY, Smith BR, Ward KW, Kopple KD. Molecular properties that influence the oral bioavailability of drug candidates. *J Med Chem*. 2002;45:2615-2623. doi:10.1021/jm020017n
31. Lipinski CA, Lombardo F, Dominy BW, Feeney PJ. Experimental and computational approaches to estimate solubility and permeability in drug discovery and development settings. *Adv Drug Deliv Rev*. 2012;64:4-17. doi:10.1016/j.addr.2012.09.019
32. Chukwuma IF, Uchendu NO, Asomadu RO, et al. African and Holy Basil – a review of ethnobotany, phytochemistry, and toxicity of their essential oil: current trends and prospects for antimicrobial / anti-parasitic pharmacology. *Arab J Chem*. 2023;16:104870. doi:10.1016/j.arabjc.2023.104870
33. Aryal S, Baniya MK, Danekhu K, Kunwar P, Gurung R, Koirela N. Total phenolic content, flavonoid content and antioxidant potential of wild vegetables from western Nepal. *Plants*. 2019;8:96-107. doi:10.3390/plants8040096
34. Ugoeze CK, Oluigbo EK, Chinko CBB. Phytomedicinal and nutraceutical benefits of the GC-FID quantified phytochemicals of the aqueous extract of *Azadirachta indica* leaves. *J Pharm Pharmacol Res*. 2020;04. doi:10.26502/fjppr.039
35. Onyesife OC, Chukwuma IF, Okagu IU, Ndefo CJ, Amujiri AN, Ogugua VN. Nephroprotective effects of *Piper nigrum* extracts against monosodium glutamate-induced renal toxicity in rats. *Sci African*. 2023;19:e01453. doi:10.1016/j.sciaf.2022.e01453
36. Orumwense GE, Osagie AM, Omega SO, Omega K, Azeke MA. *Synclisia scabrida* protects against oxidative stress, hepatotoxicity and hyperglycaemia in alloxan-induced diabetic rats. *J Diabetes Metab Disord*. 2022;21:669-680. doi:10.1007/s40200-022-01029-9
37. Chike-ekwughe A, Adegboyega AE, Johnson OT, Adebayo AH, Ogunlana OO. In vitro and in-silico inhibitory validation of *Tapinanthus cordifolius* leaf extract on alpha-amylase in the management of type 2 diabetes. *Informatics Med Unlocked*. 2023;36:101148. doi:10.1016/j.imu.2022.101148
38. Zhang P, Li T, Wu X, Nice EC, Huang C, Zhang Y. Oxidative stress and diabetes: antioxidative strategies. *Front Med*. 2020;14:583-600. doi:10.1007/s11684-019-0729-1
39. Sun C, Zhao C, Guven EC, et al. Dietary polyphenols as antidiabetic agents: advances and opportunities. *Food Front*. 2020;1:18-44. doi:10.1002/fft2.15
40. Johnson MH, de Mejia EG. Phenolic compounds from fermented berry beverages modulated gene and protein expression to increase insulin secretion from pancreatic beta-cells in vitro. *J Agric Food Chem*. 2016;64:2569-2581.
41. Egbuna C, Awuchi CG, Kushwaha G, et al. Bioactive compounds effective against type 2 diabetes mellitus: a systematic review. *Curr Top Med Chem*. 2021;21:1067-1095. doi:10.2174/1568026621666210509161059
42. Duru CE. Mineral and phytochemical evaluation of *Zea mays* husk. *Sci African*. 2020;7:e00224. doi:10.1016/j.sciaf.2019.e00224
43. Martins R, Fernandes F, Valentão P. Unearthing of the antidiabetic potential of aqueous extract of aqueous extract of *Solanum betaceum* Cav. *Leaves. Molecules*. 2023;28:3291. doi:10.3390/molecules28083291
44. Apeh VO, Asogwa E, Chukwuma FI, Okonkwo OF, Nwora F, Uke R. Chemical analysis and in silico anticancer and anti-inflammatory potentials of bioactive compounds from *Moringaoleifera* seed oil. *Adv Tradit Med*. 2022;22:59-74. doi:10.1007/s13596-020-00521-y
45. Harley BK, Kingsley B, Kingsley I, et al. *Myrianthus libericus*: possible mechanisms of hypoglycaemic action and in silico prediction of pharmacokinetics and toxicity profile of its bioactive metabolite, friedelan-3-one. *Biomed Pharmacother*. 2021;137:111379. doi:10.1016/j.biopha.2021.111379
46. Wang Y, Chen J, Song YH, et al. Effects of the resistant starch on glucose, insulin, insulin resistance, and lipid parameters in overweight or obese adults: a systematic review and meta-analysis. *Nutr Diabetes*. 2019;9:19.
47. Kajimoto T, Node M. Inhibitors against glycosidases as medicines. *Curr Top Med Chem*. 2009;9:13-33.
48. Miao F, Wansi SL, Kamani PSL, et al. In vitro α -amylase and α -glucosidase enzymes inhibitory effects of the aqueous extract of *Combretum molle* twigs. *Int J Toxicol Pharmacol Res*. 2015;7:74-79.
49. Chika A, Bello SO. Antihyperglycaemic activity of aqueous leaf extract of *Combretum micranthum* (Combretaceae) in normal and alloxan-induced diabetic rats. *J Ethnopharmacol*. 2010;129:34-37.
50. Apeh VO, Njoku OU, Nwodo FOC, Chukwuma IF, Emmanuel AA. In silico drug-like properties prediction and in vivo antifungal potentials of *Citrullus lanatus* seed oil against *Candida albicans*. *Arab J Chem*. 2022;15:103578. doi:10.1016/j.arabjc.2021.103578
51. Lawal B, Sani S, Onikanni AS, et al. Preclinical anti-inflammatory and antioxidant effects of *Azanza garckeana* in STZ-induced glycemic-impaired rats, and pharmacoinformatics of its major phytoconstituents. *Biomed Pharmacother*. 2022;152:113196. doi:10.1016/j.biopha.2022.113196
52. Apeh VO, Adegboyega AE, Chukwuma IF, et al. An in silico study of bioactive compounds of *Annona muricata* in the design of anti-prostate cancer agent: MM/GBSA, pharmacophore modeling and ADMET parameters. *Informatics Med Unlocked*. 2023;43:101377. doi:10.1016/j.imu.2023.101377
53. Yusuf AJ, Adegboyega AE, Yakubu AH, et al. Exploring *Scutellaria baicalensis* bioactives as EGFR tyrosine kinase inhibitors: cheminformatics and molecular docking studies. *Informatics Med Unlocked*. 2023;43:101406. doi:10.1016/j.imu.2023.101406
54. Chukwuma IF, Ezeorba TPC, Nworah FN, Apeh VO, Khalid M, Sweilam SH. Bioassay-guided identification of potential Alzheimer's disease therapeutic agents from kaempferol-enriched fraction of *Aframomum melegueta* seeds using in vitro and cheminformatics approaches. *Arab J Chem*. 2023;16:105089. doi:10.1016/j.arabjc.2023.105089
55. Johnson TO, Adegboyega AE, Ojo OA, et al. A computational approach to elucidate the interactions of chemicals from *Artemisia annua* targeted toward SARS-CoV-2 main protease inhibition for COVID-19 treatment. *Front Med*. 2022;9:907583. doi:10.3389/fmed.2022.907583
56. Apeh VO, Okafor KC, Chukwuma IF, et al. Exploring the potential of aqueous extracts of *Artemisia annua* ANAMED (A3) for developing new anti-malarial agents: in vivo and silico computational approach. *Eng Reports*. 2023:e12831. doi:10.1002/eng2.12831